Spectrochimica Acta Part A 78 (2011) 1027–1036

Contents lists available at ScienceDirect

Spectrochimica Acta Part A: Molecular and Biomolecular Spectroscopy

journal homepage: www.elsevier.com/locate/saa

Synthesis, structure investigation, spectral characteristics and biological activities of some novel azodyes

M.A. Zayed [a,*], Gehad G. Mohamed [a], S.A.M. Abdullah [b]

[a] Chemistry Department, Faculty of Science, Cairo University, 12613 Giza, Egypt
[b] University of Workers,10 Aswan, Egypt

ARTICLE INFO

Article history:
Received 17 September 2010
Received in revised form
25 November 2010
Accepted 10 December 2010

Keywords:
Acetoamidophenolazo compounds
UV–vis
FT-IR
^{1}H NMR
Mass spectra
MO calculations
Biological activity

ABSTRACT

Four novel azo compounds were synthesized; o-phenylazo- ($C_{14}H_{13}N_3O_2$) (I), p-bromo-o-phenylazo- ($C_{14}H_{13}BrN_3O_2$) (II), p-methoxy-o-phenaylazo- ($C_{15}H_{16}N_3O_3$) (III) and p-nitro-o-phenylazo-p-acetamidophenol ($C_{14}H_{13}N_4O_4$) (IV). These compounds were carefully investigated using elemental analyses, UV–vis, FT-IR, ^{1}H NMR and mass spectra. Also, the effects of p-substituents such as bromo, methoxy and nitro groups on the mass fragmentation pathways of these dyes were studied using Hammet's effects. This research aimed chiefly to threw lights on the structures–stability relationship of four novel newly prepared azo derivatives of p-acetoamidophenol. The data obtained referred to the variation of mass fragmentation pathways with the variation of p-substituent of these dyes which can be used in industry for various dyeing purposes. This variation is also correlated and verified by molecular orbital calculations which were done on ionic forms of these dyes using semi empirical PM3 program. The biological activities of these dyes were also investigated and its structure relationship was correlated.

1. Introduction

Recently, several studies have been published on the synthesis and spectral properties of azo dyes [1–3]. This reflects their widely important applications in different fields, such as polyester fiber [4] and disperses dyes [5], as well as their involvement in many biological reactions and in analytical chemistry [6].

Photochromic compounds are receiving more interest due to their potential applications in photonic devices such as optical memories, photo-switches, and full color displays [7–9]. The photochromic properties of the some dyes depend on several factors, such as the nature of the heteroaryl moieties, the conformation of the open-ring isomer, electron donor/acceptor substituents, and the p-conjugation length of the hetero-aryl groups, among others [10]. Electron-donating substituents can increase the absorption coefficients and decrease the cycloreversion quantum yields of some dyes, while electron-withdrawing groups do not affect the cycloreversion quantum yield but can shift the absorption maxima to longer wavelengths [11]. The longer the p-conjugation length of the hetero-aryl groups, the lower the cycloreversion quantum yields of diarylethenes [12,13]. The potential of organic dyes and their intermediates to adversely impact human health and the environment has moved toxicological considerations to the forefront of their molecular design [14].

Mass spectrometry plays pivotal role in the structural characterization of organic molecules [15]. In conjunction with mass spectrometric analysis [16,17], computational quantum chemistry can provide additional information about the atoms and bonds, which can be used successfully in an interpretation of experimental results [18].

The aim of the present work is to carry out experimental and theoretical investigation of the four azo compounds of the biological activity of p-acetamidophenol using UV–vis, FT-IR, ^{1}H NMR and EI mass spectral (MS) fragmentation at 70 eV. Also, MO calculations are performed using PM3 procedure, on the charged molecular ion to investigate bond length, bond order, heats of formation, ionization energy and charge distribution. These calculations are correlated with the EI-MS experimental results to obtain information about the stability of the studied compounds and prediction of the site of primary fragmentation step and subsequent ones. Also, it is used to discuss the effect of Hammet values of substituents on experimental and computational results. The biological activities of the azodyes under investigation are reported using *Tribolium confusum*. The structures of the azodyes (I–IV) are given in Fig. 1.

* Corresponding author. Tel.: +20 105776675; fax: +2 002 35728843/7556.
E-mail address: mazayed429@yahoo.com (M.A. Zayed).

1386-1425/$ – see front matter © 2010 Elsevier B.V. All rights reserved.
doi:10.1016/j.saa.2010.12.037

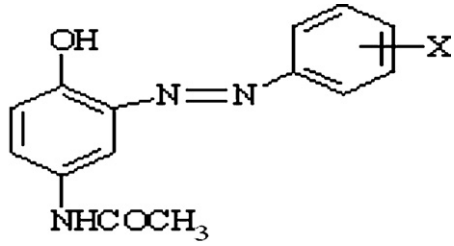

I, X = H
II, X = p-Br
III, X = p-OCH_3
IV, X = p-NO_2

Fig. 1. Structure of azodyes (I–IV).

2. Experimental

2.1. Reagents

All the chemicals used in this work were of analytical grade. They included p-acetamidophenol, aniline, p-bromoaniline, p-methoxyaniline, and p-nitroaniline (Sigma) sodium nitrite and sodium hydroxide (Adwik). Organic solvents (spectroscopic pure from BDH) used included absolute ethyl alcohol, diethylether and dichloromethane.

2.2. Preparation of dyes (I–IV)

p-Acetamidophenol-azo-derivatives (I–IV) were prepared by coupling p-acetamidophenol with aryl, p-bromo-, p-methoxy- and p-nitro-diazonium chloride, in an ice bath, in the presence of sodium hydroxide [19]. The precipitates were left in refrigerator over night, filtered and crystallized from acetic acid (yield 78–86%).

2.3. Solutions

The solutions used in UV–vis. measurements are obtained by dissolving the accurate weight of the corresponding dye in ethanol or in methylene chloride. The concentrations of the studied dyes are 0.1574×10^{-3} M, 0.126×10^{-3} M, 0.143×10^{-3} M and 0.137×10^{-2} M for dyes I, II, III and IV, respectively.

2.4. Instruments

Elemental microanalyses of the separated solid dyes for C, H and N were performed at the Microanalytical Center, Cairo University, using CHNS-932 (LECO) Vario Elemental Analyzers. The UV–vis electronic spectra of dyes (I–IV) were measured in methanol and in methylene chloride (MC) solvents using Shimadzu recording spectrophotometer UV/VIS/NIR 3101 PC model in the region of λ = 200–800 nm. The infrared spectra were recorded on a PerkinElmer FT-IR type 1650 spectrophotometer in wave number region 4000–400 cm^{-1}. The spectra were recorded as KBr pellets. ^{1}H NMR spectra were measured using an instrument of Model Gemini 2000 Switzerland using duterated dimethylsulphoxide (DMSO-d_6) and measured in Micro Analytical Center, Cairo University. Electron ionization mass spectra (EI-MS) of the studied dyes were obtained using Shimadzu GC-MS-Qp 1000 PX quadruple mass spectrometer with electron multiplier detector equipped with GC–MS data system. The direct probe (DP) for solid material was used in this study. The EI-MS spectra were obtained at ionizing energy value of 70 eV, ionization current of 60 μA and vacuum is better that 10^{-6} Torr.

The molecular orbital calculations (MOCs) were performed using semi-empirical molecular orbital calculation. The method used in these computations is the parametric method (PM3) described by Stewart [20]. The default criteria for terminating all optimizations were increased by a factor of 100 (keyword PRECISE). Vibrational frequencies were computed for the studied structures (keyword FORCE) so as to check whether the newly designed geometries are local minima. All the molecular orbital calculations were carried out at the unrestricted Hartree–Fock level (UHF) for there positively charged ions using PM-3 method followed by full optimization of all geometrical variables (bond lengths, bond angles, and dihedral angles), without any symmetry constraint. All structures were optimized to a gradient normalization of 0.01–0.05, using the eigenvector following (EF) routine [21]. All the semi empirical MO calculations were performed with the MOPAC2000 software package [22] implemented on an Intel Pentium IV 3.0 G Hz computer.

2.5. Biological activity

Adult of *T. confusum* were laboratory reared on wheat flour at 27.5 ± 1.5 °C and 70% ± 5% (R.H.) according to the method of Frederic et al. [23] with some modifications.

T. confusum adult was topically treated with 10 μm of each compound according to the protocol described by Delobel et al. [24] as follows: thirty insects divided on three replicates (10 adult/replicate) were topically and mortality was then monitored after 24 h. Thirty adults of control experiment were used in three replicates without treatment. The adult mortality was estimated according to Abbot Method [25]. Estimation of LD50 values was made using probity analysis as given by Finney [26].

3. Results and discussion

The structure elucidation of the prepared azodyes (I–IV) is carried out by using different techniques namely elemental analyses, UV–vis, FT-IR and ^{1}H NMR and mass spectroscopy, in addition to molecular orbital calculations.

The elemental analyses of the prepared dyes referred to the general formulae of o-phenylazo- ($C_{14}H_{13}N_3O_2$) (I), p-bromo-o-phenylazo- ($C_{14}H_{13}BrN_3O_2$) (II), p-methoxy-o-phenaylazo- ($C_{15}H_{16}N_3O_3$) (III) and p-nitro-o-phenylazo-p-acetamidophenol ($C_{14}H_{13}N_4O_4$) (IV) compounds, respectively.

3.1. UV–vis absorption spectra

These structures are confirmed by the UV–visible spectra in ethanol (Fig. 2a) and in methylene chloride (Fig. 2b). The correlation between the structural formulae of these dyes and the absorption spectral data is given in Table 1. The electronic transition n–π* ($\varepsilon \approx 10^3$ L mol^{-1} cm^{-1}, $\lambda_{max} \approx 330$–439 nm) generally occurs in amide carbonyl in dyes I–III together with that occurs in NO_2 group in dye IV and π–π* electronic transition ($\varepsilon \approx 10^4$ L mol^{-1} cm^{-1}, $\lambda_{max} \approx 230$–260 nm) occurs in azo group/and or other unsaturated bonds in all dyes (I–IV). These transitions in ethanol are of less molar absorptivity than in methylene chloride for all dyes. This is may be attributed to the effect of polarity difference of the two solvents. The position of their bands (Fig. 2) is varied from one dye to the other and from one solvent to another which may be attributed to the p-phenylazo substituent variable donating power.

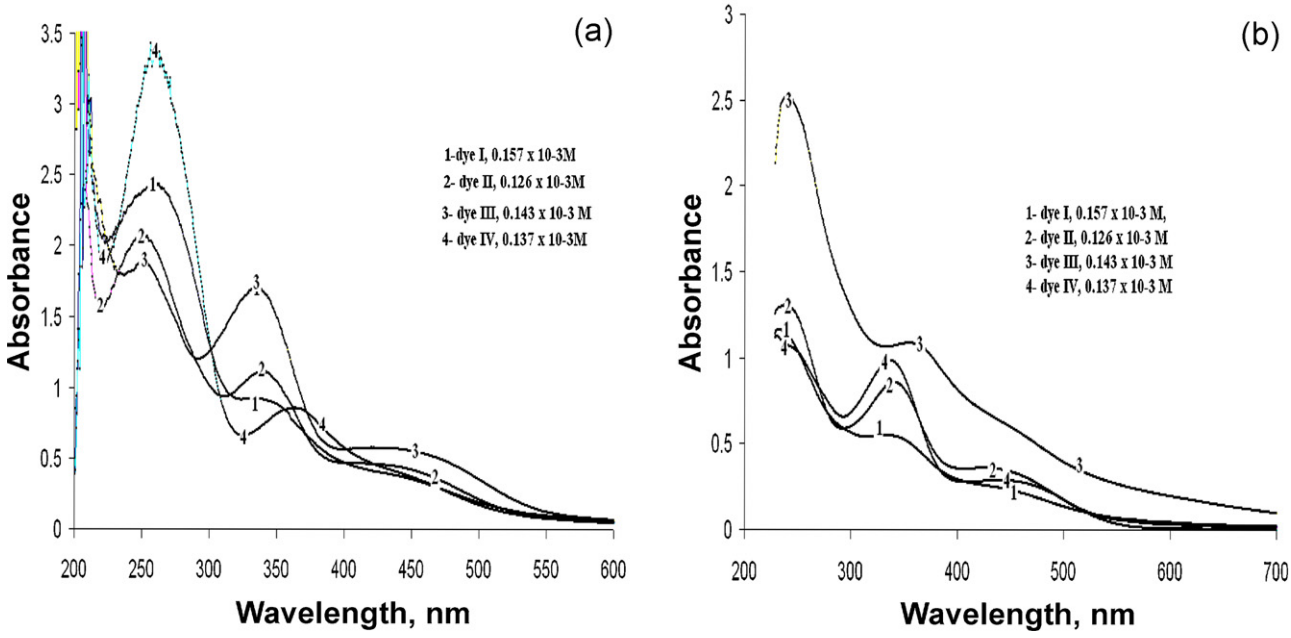

Fig. 2. (a) The absorption spectra of dyes I–IV in ethonal. (b) The absorption spectra of dyes I–IV in methylene chloride.

3.2. Infrared spectral studies

FT-IR spectra (Fig. 3) of these dyes are correlated with their proposed structural formulae (Table 2). These data refer to assignment of main bands of the active groups in the moiety of these dyes, such as 510–618, 1173–1310, 1419–1595, 1657, 3028–3056 and 3284–3560 cm^{-1} for ν(C–N) amide, ν(C–O) amide, $\nu(CH_3)$ amide, ν(N=N azo), ν(CO) amide, ν(NH amide) and ν(OH phenolic) in dyes (I–IV), respectively. The positions of these bands are varied from one dye to another due to the variation of donating power effect of p-substituent of phenyl azo group. Extra bands are appeared at 515–585 cm^{-1} for νC–Br in case of dye II and 832 cm^{-1} of νNO_2 in case of dye IV.

3.3. ^1H NMR spectra

The ^{1}H MNR spectra of these dyes (I–IV) are given in Table 3. These ^{1}H NMR data are correlated with the proposed structures of these dyes. In dye I (Fig. 4), the chemical shifts appeared at δ = 1.700–2.502, 3.416–4.000, and 7.056–7.707 are attributed to protons of CH_3, NH and OH of acetamidophenol, aromatic, protons of phenylazo group, and aromatic protons of phenyl group of acetamidophenol, respectively. The main proton chemical shifts of other dyes (II–IV) appeared at different values depending upon the donating power effect of p-substituent of p-phenylazogroups. These δ values are appeared in case of dye II, at 7.606–7.767 of aromatic protons of p-Br-phenylazo group; and in case of dye III, at

Table 1
The UV–vis spectral data description of a – 2 ml of 0.01 g/ml ethanol, b – 2 ml of 0.01 g/ml methylene chloride of some acetoamidophenolazo derivatives (I–IV).

Compound	λ_{max} (nm)	Absorbance	ε (L mol^{-1} cm^{-1})	Electronic transition
I, 0.1574×10^{-3} M	a – 333.5	a-0.9214	5.853×10^3	n–π* in CO group
	260.5	2.4440	1.552×10^4	π–π* in azo group
	b – 333.4	b – 0.5460	3.46×10^3	n–π* in CO group
	231.0	1.1659	0.74×10^4	π–π* in azo group
II, 0.126×10^{-3} M	a – 338.5	a – 1.1135	8.83×10^3	n–π* in CO group
	251.0	2.0793	1.65×10^4	π–π* in azo group
	b – 340.5	b – 0.8574	6.8×10^3	n–π* in CO group
	238.5	1.3026	1.033×10^4	π–π* in azo group
III, 0.143×10^{-3} M	a – 363.0	a – 0.8537	5.97×10^3	n–π* in CO group
	256.5	3.4323	2.40×10^4	π–π* in azo group
	b – 355.0	b – 1.0859	7.59×10^3	n- π* in CO group
	237.0	2.5099	1.75×10^4	π–π* in azo group
IV, 0.137×10^{-2} M	a – 420.5	a – 0.5730	4.18×10^3	n–π* in CO group
	334.5	1.6976	1.23×10^4	π–π* in azo group
	250.5	1.8818	1.37×10^4	π–π* in NO_2 group
	b – 439.5	b – 0.2860	2.08×10^3	n–π* in CO group
	337.0	0.9830	0.717×10^4	π–π* in azo group
	230.5	1.1261	0.821×10^4	n–π* in NO_2 group

I—o-phenylazo-pacetamedophenol, II—p-bromo-o-phenylazo-p-acetamedophenol, III—p-methoxy-o-phenylazo-p-acetamedophenol, IV—p-nitro-o-phenylazo-p-acetamedophenol.

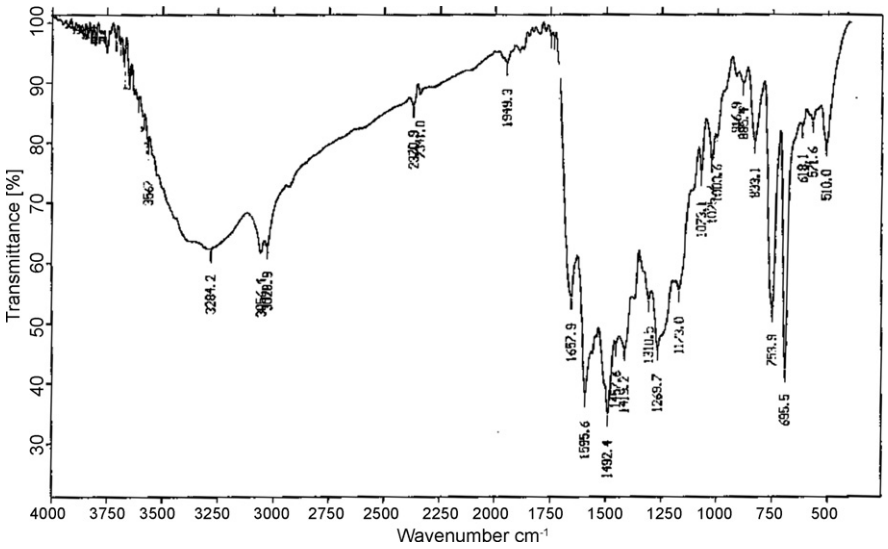

Fig. 3. The FT-IR spectra of dye I.

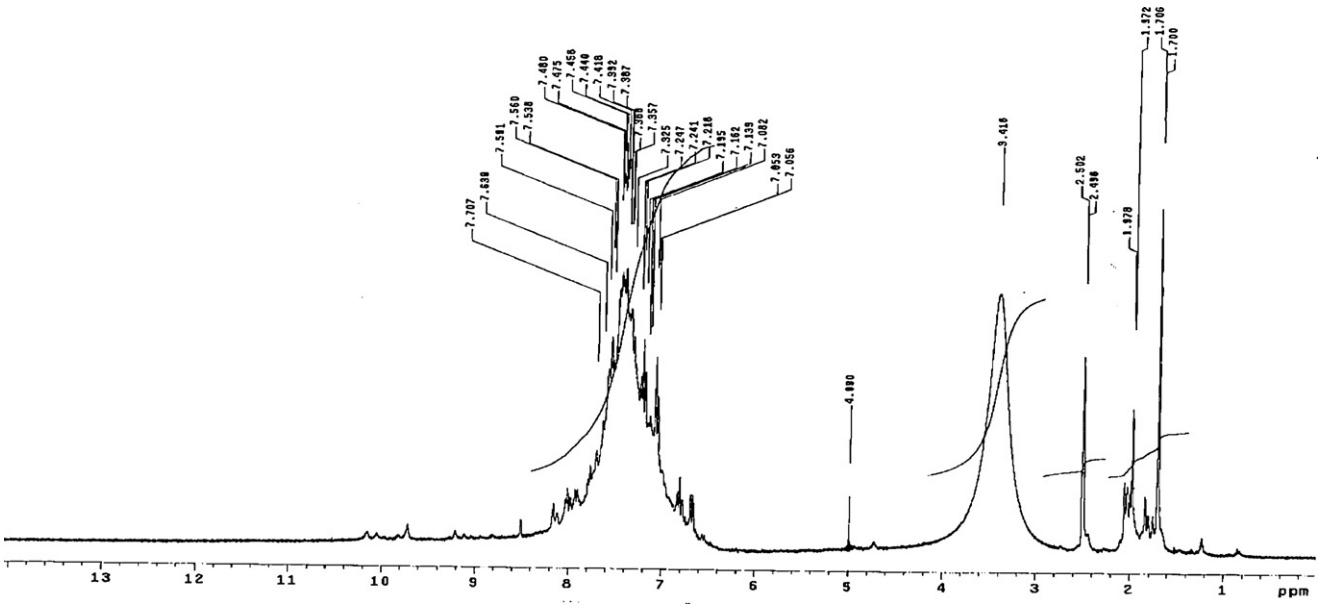

Fig. 4. The ^{1}H NMR spectra of dye I.

1.674–2.502 of CH_3 protons of aliphatic CH_3O; in case of dye IV at 8.182–8.43 of aromatic protons of p-NO_2-phenylazo group.

3.4. Mass spectral fragmentation

Knowledge of the decomposition mechanisms of these dyes is very important to understand its chemical structure–reactivity relationship. It is difficult to establish the exact major fragmentation pathway in EI using conventional MS. However, combination of the experimental techniques (UV–vis, FT-IR, ^{1}H NMR and MS) and MO calculations is very important to understand the following topics:

1. Primary site fragmentation process and its major fragmentation pathway.
2. Stability of the studied dyes as positively charged molecules in solid state phase and molecular ions in gas phase.
3. Selection of the most probable decomposition pathways in vitro system using MS technique.
4. Substituent effects on experimental and computational results.

Electron ionization (EI) mass spectra of the four dyes (I–IV) at 70 eV were recorded and investigated (e.g. of dye I, Fig. 5). The proposed of principal and important fragmentation pathways following electron impact is shown in Schemes 1–4. The signal

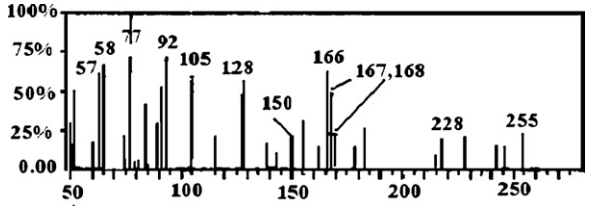

Fig. 5. EI-MS of dye I.

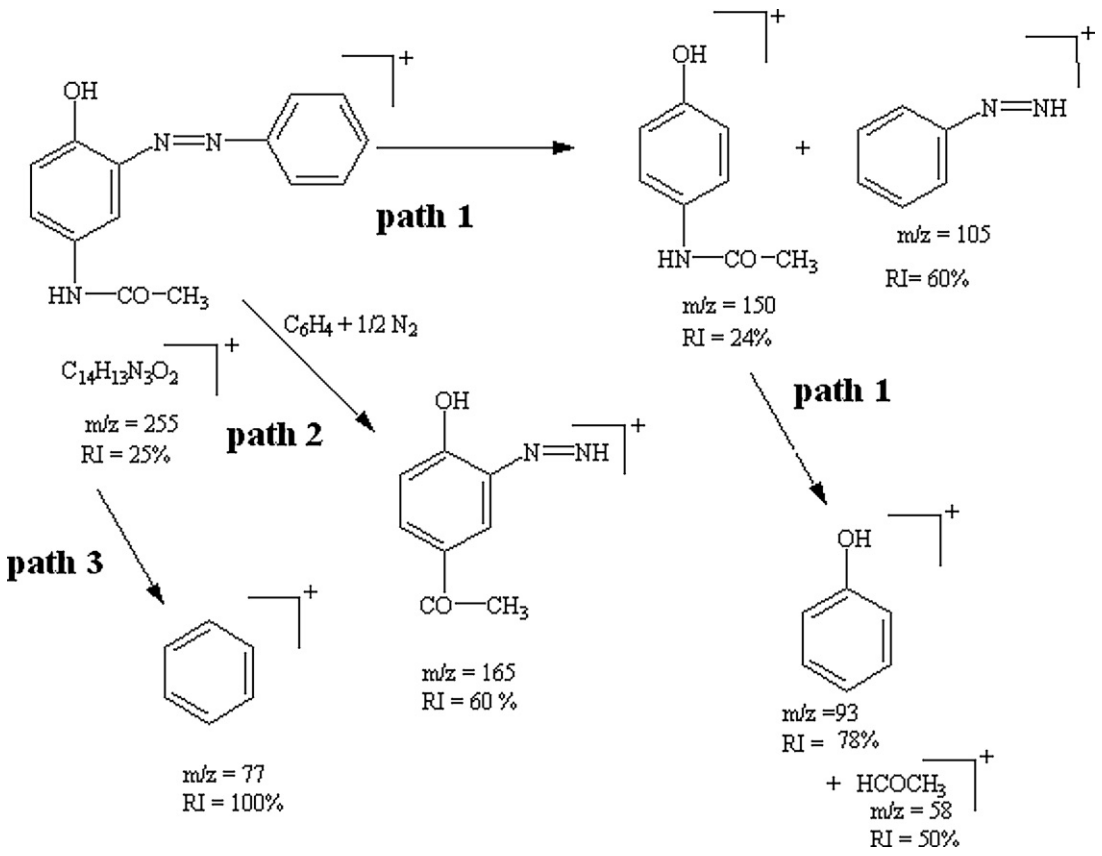

Scheme 1. Mass spectral fragmentation pathways of dye I.

appeared in the mass spectra of dyes I, II, III and IV at $m/z = 255$, 333, 286 and 300 are due to the formation of molecular ions, ($C_{14}H_{13}N_3O_2^+$, RI = 25%), ($C_{14}H_{13}N_3O_2Br^+$, RI = 24%), ($C_{15}H_{16}N_3O_3^+$, RI = 20%) and ($C_{14}H_{13}N_4O_4^+$, RI = 15%) for these dyes, respectively. The appearance of these molecular ions confirms their proposed general formula and agrees well with their elemental analyses. In case of dye I (Scheme 1) mass spectra (Fig. 5) refer to the appearance of mole fragments in three pathways. The signals appeared at $m/z = 58$ (RI = 50%) due to fragment ion $HCOCH_3$, 77 (RI = 100%, base peak) due to fragment ion C_6H_5 and the fragment ions containing

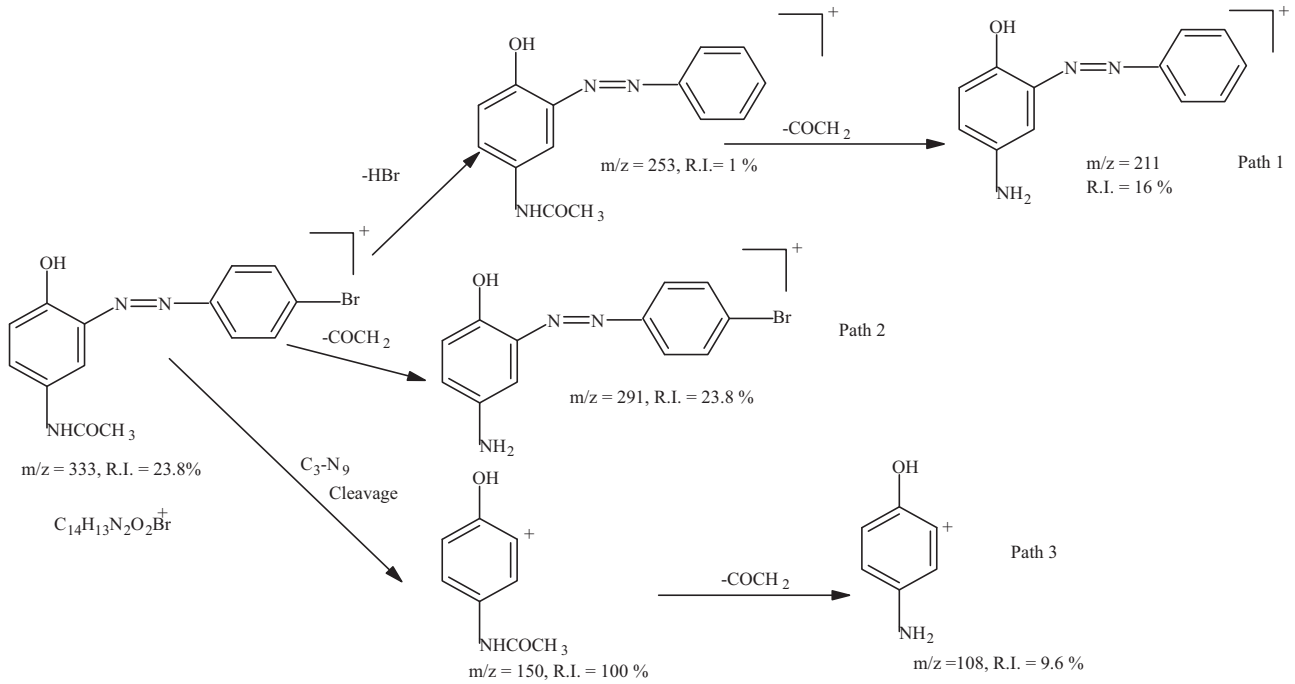

Scheme 2. The mass spectral fragmentation pathways of the dye II.

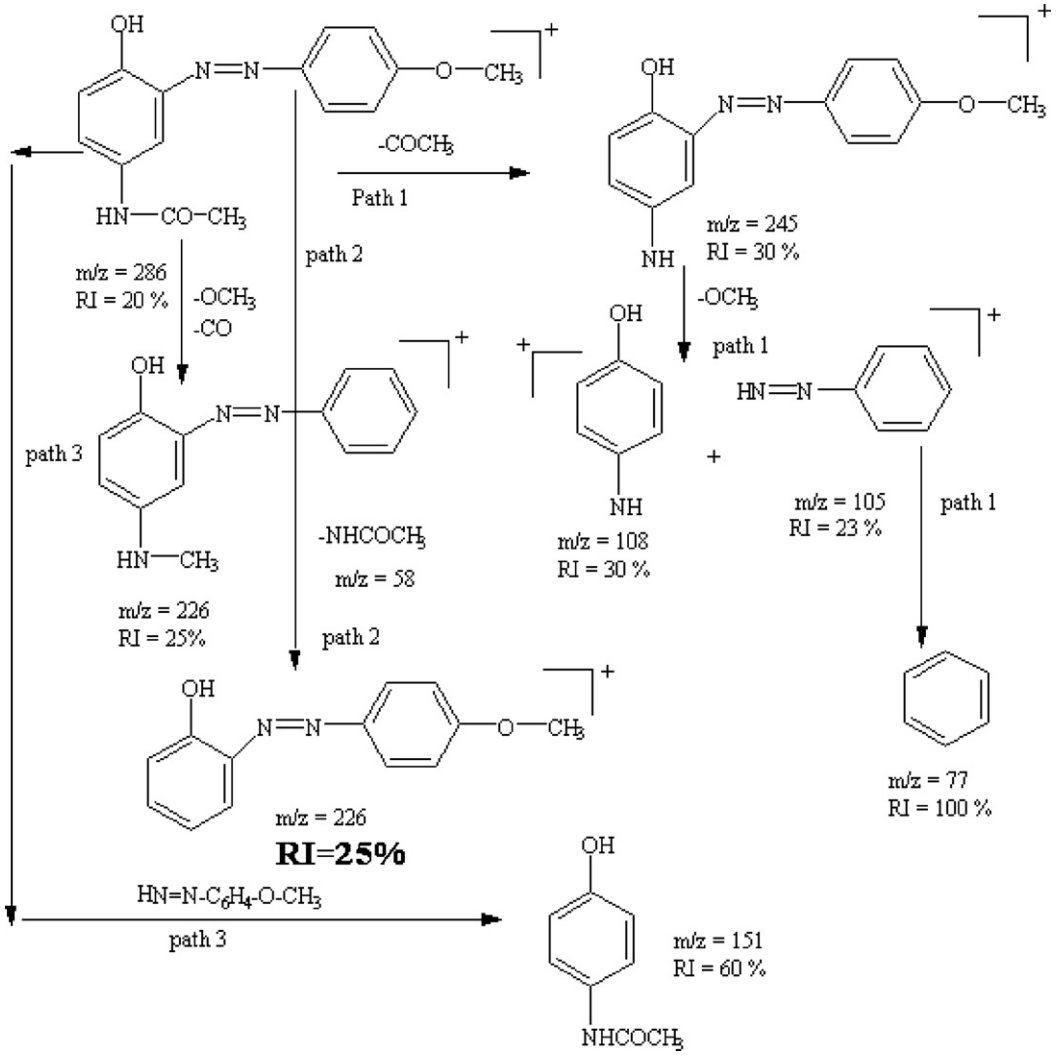

Scheme 3. Mass fragmentation scheme of dye III.

azo group appeared at $m/z = 105$ (RI = 60%) due to C_6H_5–N=NH, and at 165 (RI = 60%) due to CH_3CO–C_6H_4 (OH)–N=NH. The appearance of the fragment ions containing azo group of high RI of 60% refer to the stability of azodye I even at high energy ionization source 70 eV. In case of dye II (Scheme 2) its mass spectra show fragmentation of this dye in three parallel pathways. It shows in path I, fragment ions at $m/z = 253$ (RI = 1%) after the loss of HBr from the molecular ion; at $m/z = 211$ (RI = 16%) due fragment ion containing azo group; at $m/z = 291$ (RI = 30%) in path containing also azo group; and at $m/z = 150$ (RI = 100%; base peak) containing no azo group. The low RI values of fragment ions containing azo group may refer to the low stability of p-bromoazodye II on its ionization with the high energy electron beam of 70 eV. In case of p-methoxy azo dye III mass, its fragmentation occurs in three pathways as given by Scheme 3. It shows three fragment ions containing azo group of $m/z = 245$ (RI = 30) and $m/z = 105$ (RI = 23%) in path 1; $m/z = 226$ (25%) in both paths 2 and 3. The middle values of RI % of these fragment ions containing azo group may refer to the middle stability of p-methoxyazo dye III. It is finally decomposed to give the fragment ion of $m/z = 151$ (RI = 60%) of p-acetamidophenol parent compound and $m/z = 77$ (RI = 100%) as a base peak of $C_6H_5^+$ stable fragment ion. The EI-MS of p-nitroazodye IV, are explained in Scheme 4. It shows three fragmentation pathways. This scheme shows three fragment ions containing azo groups. These are at $m/z = 254$ (RI = 1%), at $m/z = 212$ (RI = 28%) in path 1 and at $m/z = 258$ (RI = 12.5%) in path 2. The last one fragment ion is the only one containing p-nitro-azo group. The lower RI% values may refer to the instability of p-nitro-azodye IV in a similar way like p-bromoazodye II. This means that the electron withdrawing substituents are weakening the azodye stability. This also confirmed by its absorption spectra at longer wavelengths than the main azo dye I. Therefore, we may order the stability of these dye during ionization with 70 eV electron beam as dye I > dye III > dye II > dye IV. This is agrees well with the Hammet values in relation to some MOCs parameters such as heat of formation, dipole-moment, electron affinity and ionization potential (Table 4).

3.5. MO calculations

Molecular orbital calculations (Tables 4–8) give valuable information about the structure and the reactivity of a molecule and its molecular ions. Computational data can be used to support the experimental data. The much import parameters calculated using MO calculation are geometries, bond order, bond strain, charge distribution, heat of formation and ionization energy. Investigation of the molecular structure of four dyes I–IV was interest in the present work aiming to help in illumination of experimental data (i.e. prediction of the weakest bond cleavage and the stability of the cationic forms of these dyes). The weakness of the bond is indicated by its longer bond length, by the less value of the bond order and the high value of bond strain and vise versa.

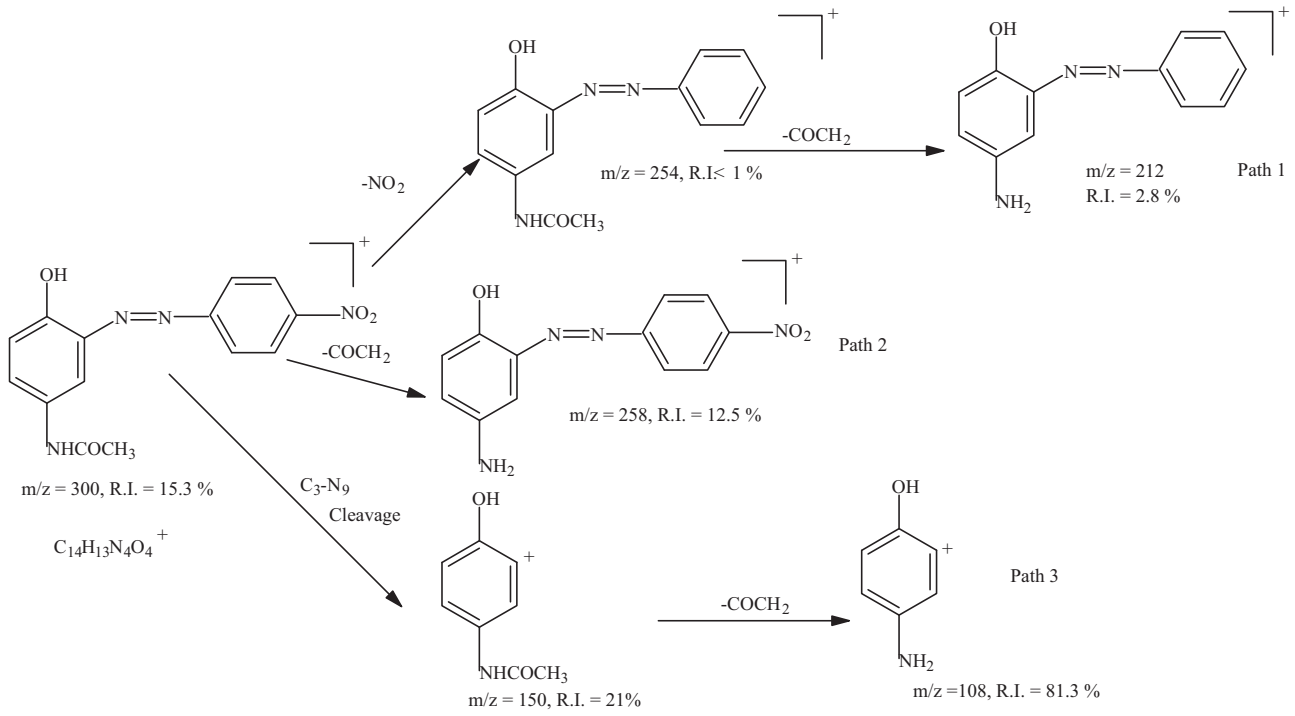

Scheme 4. The mass spectral fragmentation pathways of the dye IV.

Fig. 6 shows the numbering system of the dyes I–IV skeleton that helps in ordering the calculated bond order and charge distribution (of different atoms) of the charged species. The calculated geometrical parameters are shown in Tables 4–8. From the calculated geometries (dipole moment, heat of formation, ionization potential, Table 4) and (bond length, and bond order) for dye I (Table 5) it is clear that the order of increasing stability of bonds is: C16–C17 < N11–C16 < C3–N9 < N13–C19 < C5–N11 < N9–N13.

Table 2
The FT-IR spectral data description of acetoamidophenolazo derivatives (I–IV).

Compound	Wave number (cm^{-1})	Description
I	510–618	νC–N amid, C–O amid
	1173–1310	νCH_3 amid
	1419–1595	νN=N azo
	1657	νCO amid
	3028–3056	νOH phenolic
	3284–3560	νNH amid
II	515–585	νC–Br, νC–O amid
	1007–1068	νCH_3 amid
	1420–1664	νN=N
	1663	νCO amid
	3087	νOH phenolic
	3284–3684	νNH amid
III	511–585	νC–N amid, νC–O
	1105–1203	νCH_3 amid
	1426–1666	νN=N
	1666	νCO amid
	3108	νOH phenolic
	3321–3648	νNH amid
IV	522–640	νC–O amid, νN–O
	832	νNO_2
	1176–1293	νCH_3 amid
	1660	νCO amid
	1439–1660	νN=N
	2835–3069	νOH phenolic
	3291–3600	νNH amid

I—o-phenylazo-pacetamedophenol, II—p-bromo-o-phenylazo-p-acetamedophenol, III—p-methoxy-o-phenylazo-p-acetamedophenol, IV—p-nitro-o-phenylazo-p-acetamedophenol.

Table 3
The ^1H NMR spectral data description of some p-acetoamidophenolazo derivatives (I–IV).

Compound	Chemical shift values, σ	Description
I	1.700–2.502	Protons of CH_3 of acetamidophenol
	3.416–4.000	Protons of NH and OH of acetamidophenol
	7.056–7.366	Aromatic protons of phenylazo group
	7.357–7.707	Aromatic protons of phenyl group of acetamidophenol
II	2.024–2.497	CH_3 protons of acetamidophenol group
	3.00–4.00	Protons of NH and OH groups of acetamidophenol
	7.606–7.767	Aromatic protons of p-Br-phenylazo group
	9.900–10.300	Aromatic protons of phenyl group of acetamidophenol
III	1.674–2.502	CH_3 protons of aliphatic CH_3O
	3.372–3.904	CH_3 protons of acetamido group
	6.672–7.175	Protons of phenolic and of NH amid group
	7.197–8.038	Protons of substituted phenylazo group
	9.903–10.303	Aromatic protons of acetamidophenol
IV	2.035–2.500	CH_3 protons of acetamido group
	7.048–8.058	Protons of NH and OH of acetamidophenol
	8.182–8.436	Aromatic protons of p-NO_2-phenylazo group
	9.955–10.639	Aromatic protons of acetamidophenol

I—o-phenylazo-pacetamedophenol, II—p-bromo-o-phenylazo-p-acetamedophenol, III—p-methoxy-o-phenylazo-p-acetamedophenol, IV—p-nitro-o-phenylazo-p-acetamedophenol.

Table 4
The MOCs parameters and Hammet's subtituents values of dyes I–IV.

The dye no. and state	Heat of formation (kcal/mol)	Dipole moment (Debye)	Electron affinity (eV)	Ionization potential (eV)	Hammet constant
I, p-H Cationic state	184.37137	6.160	4.421	12.71	0.01
II, p-Br Cationic state	193.633	15.942	4.482	12.78	0.23
III, p-OCH_3Cationic state	144.964	8.707	4.333	12.62	−0.27
IV, p-NO_2 Cationic state	181.990	17.920	4.705	13.03	0.78

This means that the first cleavage bond is C16–C17 followed by N11–C16, C3–N9 and N13–C19. The most stable bonds are azo group (N9–N13) and its neighbor bond C5–N11. The calculated geometries of the cationic form of dye II (Table 6) refer to the order of increasing stability of bonds is: C22–Br25 < C16–C17 < N11–C16 < C3–N9 < N13–C19 < C5–N11 < N9–N13. This means that the first cleavage bond is C22–Br25, C16–C17 followed by N11–C16, C3–N9 and N13–C19. The most stable bonds are azo group (N9–N13) and its neighbor bond C5–N11. Also there is highly stable bond C16–O18. In case of dye III, the geometries (Table 7) indicate that, the order of increasing stability of bonds is: N11–C16 < C16–C17 < O25–C26 < C3–N9 < N13–C19 < C5–N11 < N9–N13. This means that the first cleavage bond is N11–C16 and C16–C17 followed by O25–C26, C3–N9 and N13–C19. The most stable bonds are azo group (N9–N13) and its neighbor bond C5–N11. Also there is another stable bond C16–O18. The molecular orbital geometries of dye IV (Table 8) indicate that, the order of increasing stability of bonds is: C22–N25 < N11–C16 < C16–C17 < N13–C19 < C3–N9 < N9–N13. This means that the first cleavage bond is C22–N25 followed by N11–C16, C16–C17, C3–N9 and N13–C19. The most stable bonds are azo group (N9–N13) and its neighbor bond C5–N11. Also there are other stable bonds C16–O18, N25–O38 and N25–O37 of nitro group.

3.6. Comparison between EI-MS and MO calculations

The scope of the present investigation is restricted to a search or prediction and discerns features of initial bond ruptures during the course of fragmentation of dyes (I–IV) molecules. Empirical observations indicate that the course of subsequent fragmentation is determined to large extent by the initial bond ruptures of the molecular ion in MS [26]. It is quite acceptable to say that the computational quantum chemistry can provide additional data which can be used successfully to interpret MS experimental results. These theoretical data can, particularly, be valuable for mass spectrometry scientists; in which the gas-phase species can be handled much more easily by quantum chemistry than those surrounded by solvent [27].

Comparing computational data and the previously EI-MS of dyes I–IV indicate that, dye I fragmentation starts with the cleavage of C3–N9 to give m/z = 105 (RI = 60%) containing phenylazo group and m/z = 150 (RI = 24%) of p-acetamidophenol parent, followed by the rupture of C16–N11, in path 1. In path 2 it starts its fragmentation with C19–N13 and C3–N9 bonds cleavage leading to the formation of fragment ion of m/z = 165 (RI = 60%) containing azo group. Also path 3 refer to the cleavage of bond C19–N13 to give the most abundant fragment of m/z = 77 (RI = 100%). The geometries also refer to the highest stable bond is the azogoup. This conclusion agree well with mass, UV–vis, and IR data, that dye I is the most stable dye (heat of formation = 184.37 kcal/mol). Dye II in path 1 also starts its mass fragmentation by the weakest bond C22–Br25 leading to phenylazoacetamidophenol of m/z = 253 (RI = 1%), followed by the rupture of the bond C16–N11 to form a fragment

Table 5
The calculated geometries of dye I in cationic state.

Dye I, cation, p-H					
Atom	Atom ID	Partial charge	Bond	Bond length (Å)	Bond order
O8	8	−0.128	C2–O8	1.326	1.229
N9	9	−0.016	C3–N9	1.442	1.035
N11	11	0.193	C5–N11	1.375	1.303
N13	13	0.081	N9–N13	1.230	1.898
C16	16	0.252	N11–C16	1.471	0.947
C17	17	−0.143	C16–C17	1.499	0.959
O18	18	−0.278	C16–O18	1.211	1.899
C19	19	−0.145	N13–C19	1.435	1.037

Table 6
The calculated geometries of dye II in cationic state.

Dye-II-cation, p-Br					
Atom	Atom ID	Partial charge	Bond	Bond length (Å)	Bond order
O8	8	−0.128	C2–O8	1.326	1.229
N9	9	−0.014	C3–N9	1.443	1.031
N11	11	0.196	C5–N11	1.374	1.307
N13	13	0.075	N9–N13	1.229	1.903
C16	16	0.252	N11–C16	1.471	0.944
C17	17	−0.143	C16–C17	1.498	0.959
O18	18	−0.276	C16–O18	1.211	1.901
C19	19	−0.138	N13–C19	1.437	1.034
Br25	25	0.060	C19–C24	1.405	1.367
H30	30	0.086	C22–Br25	1.863	0.984

Table 7
The calculated geometries of dye III in cationic state.

Dye-III-cation (p-methoxy)					
Atom	Atom ID	Partial charge	Bond	Bond length (Å)	Bond order
O8	8	−0.128	C2–O8	1.326	1.226
N9	9	−0.032	C3–N9	1.439	1.040
N11	11	0.188	C5–N11	1.376	1.295
N13	13	0.097	N9–N13	1.232	1.875
C16	16	0.252	N11–C16	1.469	0.950
C17	17	−0.143	C16–C17	1.499	0.959
O18	18	−0.280	C16–O18	1.211	1.895
C19	19	−0.196	N13–C19	1.429	1.054
C26	26	0.047	C22–O25	1.369	1.081
H27	27	0.036	O25–C26	1.410	0.979

Table 8
The calculated geometries of dye IV in cationic state.

Dye-IV cat, p-nitro					
Atom	Atom ID	Partial charge	Bond	Bond length (Å)	Bond order
N9	9	0.003	C3–N9	1.446	1.023
N11	11	0.205	C5–N11	1.373	1.318
N13	13	0.057	N9–N13	1.228	1.923
C16	16	0.252	N11–C16	1.474	0.938
C17	17	−0.143	C16–C17	1.498	0.959
O18	18	−0.271	C16–O18	1.210	1.905
C19	19	−0.082	N13–C19	1.443	1.019
H30	30	0.086	C22–N25	1.512	0.879
H31	31	0.087	N25–O37	1.212	1.518
H32	32	0.107	N25–O38	1.212	1.517

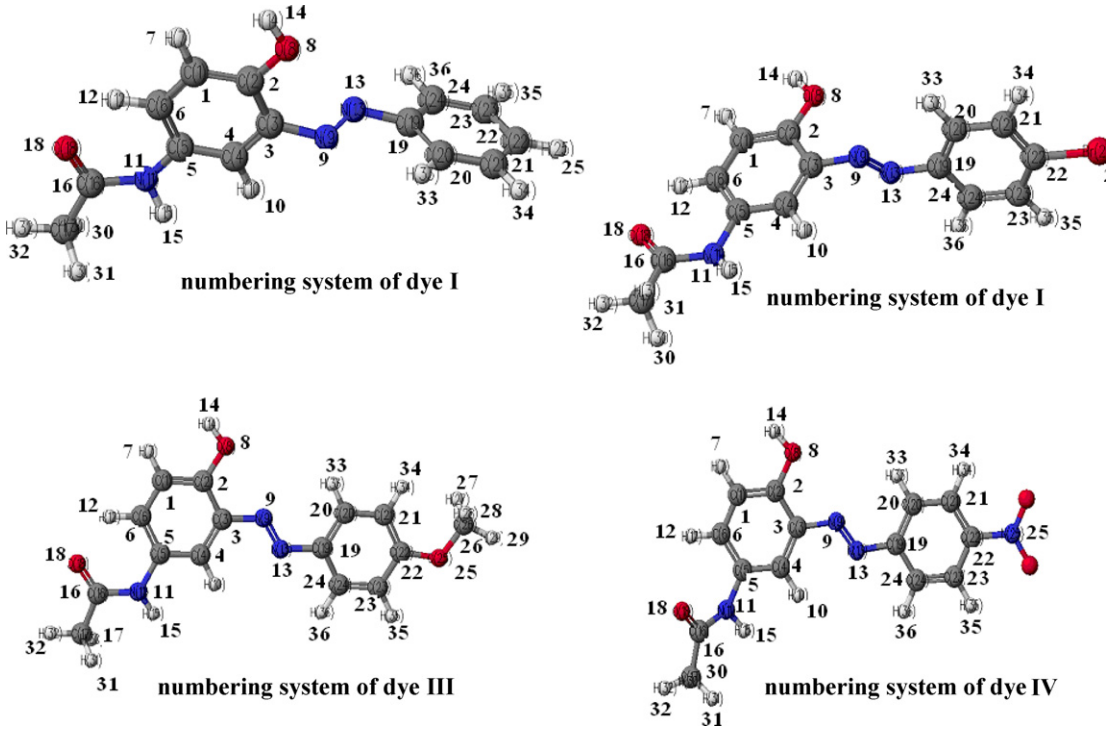

Fig. 6. Numbering systems of dyes I–IV.

of m/z = 211 (RI = 16%) containing azo group. In path 2, dye II starts its decomposition by the rupture of C16–N11 to form a fragment ion containing azo group of m/z = 291 (RI = 21.8%). In path 3, dye II gives the most abundant p-acetamidophenol parent fragment of m/z = 150 (RI = 100%) via the rupture of the C3–N9 bond and this is followed by the rupture of the bond C16–N11 to form a fragment ion of m/z = 108 (RI = 9.6%) of p-aminophenol. The computational data also refer to the high stability of the azo bond N9–N13 (heat of formation of dye II = 193.63 kcal/mol), but unfortunately the presence of Br substituent facilitates the azo group decomposition in path 3. It also makes the dye II less stable than dye I. Dye III in path 1 starts its decomposition by the rupture of the weak bond C16–N11 to give p-methoxy-phenylazo fragment ion of m/z = 245 (RI = 30%) followed by the loss of p-methoxy group via the rupture of the second weak bond C22–O25 to give a fragment ion of m/z = 105 (RI = 23%) and finally it gives the most abundant fragment ion of m/z = 77 (RI = 100%) in the same way like dye I. In path 2, dye III still keeping the p-methoxy group after rupture of the bond C5–N11 leading to the formation of the fragment ion of m/z = 226 (RI = 25%). In path 3, the dye III loosed the p-methoxy-phenylazo group via the rupture of the weak bond C3–N9 leaving the parent fragment ion of p-acetoamidophenol of m/z = 151 (RI = 60%). This comparison conclude that dye III (heat of formation = 144.96 kcal/mol) is more stable than dye II and less stable than dye I. Dye IV mass shows three pathways, it starts in path 1 with cleavage of the bond C22–N25 by loss of NO_2 group leading to the formation of low abundant fragment ion of dye I of m/z = 254 (RI = 1%), it follows with the rupture of the bond C16–N11 leading to the formation of fragment ion still containing azo group of m/z = 212 (RI = 28%). In path 2, the fragment ion containing azo group of m/z = 258 (RI = 12.5%) is formed via the rupture of C16–N11, keeping the NO_2 in its entity. Therefore, the presence of NO_2 decreases abundance of this azo fragment ion if compared with that of m/z = 212 fragment ion free from this group. In path 3, dye IV gives the parent p-acetoamidophenol fragment ion of m/z = 150 (RI = 21%) by the loss of p-nitro-phenylazo group and cleavage of the weak bond C3–N9. Therefore, we can conclude that the presence of NO_2 decreases abundance of azo fragment ions and consequently dye IV stability (heat of formation = 181.99 kcal/mol). Consequently comparison of practical mass results of dyes with theoretical MOCs facilitates to understand stability of these compounds, fragmentation pathways, and the bond cleavage order of each dye.

Table 9
Effect of the phenylazo compounds on the *Tribolium confusum*.

Phenyazo compounds				
%Conc.	Dye III (p-OCH_3)	Dye IV (p-NO_2)	Dye II (p-Br)	Dye I (p-H)
10	15	12	38	9
30	40	30	100	20
50	68	55	00	36
LC_{50}	36	48	15	64
Control	00	00	00	00

3.7. The biological activities of dyes

The biological activity of four dyes was studied and data obtained are represented in Table 9. From these data it concluded that [28–33] the dye II (P–Br) is the most biologically active dye where it produced 38 and 100% mortalities of the *T. confusum* at concentration of 10 and 30%, respectively. The same previous two concentrations of the dye III (p-OCH_3) caused 15 and 40 mortalities of adult *T. confusum*; the dye IV (p-NO_2) caused 12 and 30 mortalitis and finally the dye I (p-H) caused 9 and 20 of *T. confusum* mortality, respectively. On the other hand the most effective concentration was 30 in case of dye II while the concentration of 50% was the highest bioactive in case of dye III, dye IV and dye I, respectively. In order of toxicity, LC_{50} of the phenylazo compounds was 36, 48, 15 and 64 of the dye III, dye IV, dye II and dye I, respectively. It is finally concluded that presence of p-substituent near to the azo group make the dye biologically active. The order of reactivity of these dyes is more or less the reverse of their stability.

4. Conclusion

This work provides an application of various spectroscopic techniques for structure elucidation of four novel acetoamidophenol azodyes I–IV. Also, computational investigation is applied using semi-empirical MO-calculations (PM3 procedure) on cationic species of these compounds I–IV. From the mass results and MOCs data, it is concluded that the order of the stability of these dyes during ionization with 70 eV electron beam is: dye I > dye III > dye II > dye IV. The values of Hammet substituent constants (Table 4) support this order. Consequently comparison of practical mass results of dyes with theoretical MOCs facilitates to understand stability of these compounds, fragmentation pathways, and the bond cleavage order of each dye. These data can be used in industrial applications of these dyes in mordant dying processes. From the biological activity studies it is also concluded, that the order of reactivity of these dyes is more or less the reverse of their stability.

References

[1] Z. Xin, F. Sanda, T. Endo, Synthesis and characterization and coloured monomersbased on 2-methyresorcinol, Dyes Pigments 49 (2001) 1–7.
[2] A. Ni, K. Chen, H. Tian, Synthesis of heteroaryl pyridone methane dye, Dyes Pigments 50 (2001) 13–19.
[3] J. Koh, A.J. Greaves, Synthesis and application of an alkali-clearable azo disperse dye containing a fluorosulfonyl group and analysis of its alkali-hydrolysis kinetics, Dyes Pigments 50 (2001) 117–126.
[4] S. Tauro, E. Coutinho, Azo, hydrazone and other tautomers of the azo dye 7-amino-4-hydroxy-3-[(4-methoxy-2-sulfophenyl)azo]-2-naphthalenesulfonic acid: a PM3 study, J. Mol. Struct. (Theochem.) 532 (1–3) (2000) 23–39.
[5] S.S. Kandil, Cobalt(II), nickel(II) and copper(II) complexes of 4-(sulfonylazido) phenyl-azopyrazolones, Transition Met. Chem. 23 (1998) 461–465.
[6] H.B. Hassib, S.A. Abdel-latif, Potentiometric, spectrometric, thermal and conductimetric studies on some 3-phenyl-4-(arylazo)-5-pyrazolones and their complexes with divalent cobalt metal ion, Spectrochim. Acta 59A (11) (2003) 2425–2434.
[7] H. Dürr, H. Bouas-Laurent, Photochromism, Molecules and Systems, Elsevier, Amsterdam, 1990.
[8] H. Tian, Y.L. Feng, Next step of photochromic switches, J. Mater. Chem. 18 (2008) 1617–1622.
[9] K. Higashiguchi, K. Matsuda, N. Tanifuji, M. Irie, Full-color photochromism of a fused dithienylethene trimer, J. Am. Chem. Soc. 127 (2005) 8922–8923.
[10] K. Yumto, M. Irie, K. Matsuda, Control of the photoreactivity of diarylethene derivatives by quaternarization of the pyridylethynyl group, Org. Lett. 10 (2008) 2051–2054.
[11] M. Irie, K. Sakemura, M. Okinaka, K. Uchida, Photochromism of dithienylethenes with electron-donating substituents, J. Org. Chem. 60 (1995) 8305–8309.
[12] M. Irie, T. Eriguchi, T. Takada, K. Uchida, Photochromism of diarylethenes having thiophene oligomers as the aryl groups, Tetrahedron 53 (1997) 12263–12271.
[13] A.T. Bens, D. Frewert, K. Kodatis, C. Kryschi, H.D. Martin, H.P. Trommsdorff, Coupling of chromophores: carotenoids and photoactive diarylethenes-photoreactivity versus radiationless deactivation, Eur. J. Org. Chem. (1998) 2333–2338.
[14] M.A. Brown, S.C. Devito, Predicting azo dye toxicity, Crit. Rev. Environ. Sci. Technol. 23 (3) (1993) 249–324.
[15] E.H. Kerns, R.A. Rourich, K.J. Volk, M.S. Lee, Buspirone metabolite structure profile using a standard liquid chromatographic-mass spectrometric protocol, J. Chromatogr. B 698 (1997) 133–145.
[16] S. Bourcier, Y. Hoppilliard, Fragmentation mechanisms of protonated benzylamines. Electrospray ionisation-tandem mass spectrometry study and ab initio molecular orbital calculations, Eur. J. Mass Spectrom. 9 (2003) 351–360.
[17] M.A. Fahmey, M.A. Zayed, H.G. El-Shobaky, Study of some phenolic-iodine redox polymeric products by thermal analyses and mass spectrometry, J. Therm. Anal. Calorim. 82 (2005) 137–142.
[18] M.A. Zayed, M.A. Fahmey, M.F. Hawash, A.A. El-Habeeb, Mass spectrometric investigation of buspirone drug in comparison with thermal analyses and molecular orbital calculations, Spectrochem. Acta A67 (2007) 522–530.
[19] G.G. Mohamed, Ph.D. thesis, Potentiometric and spectrophotometric studiers on chemical behavior of acetamidophenol drugs with bromine. Cairo University, 1996.
[20] J.J.P. Stewart, Optimization of parameters for semiempirical methods. III. Extension of PM3 to Be, Mg, Zn, Ga, Ge, As, Se, Cd, In, Sn, Sb, Te, Hg, Tl, Pb, and Bi, J. Comput. Chem. (1991) 12320–12341.
[21] J. Baker, An algorithm for the location of transition states, J. Comb. Chem. 7 (4) (2004) 385–395.
[22] J.J.P. Stewart, MOPAC 2000, Fujitsu Limited, Tokyo, Japan, 1999.
[23] G. Frederic, R. Isabelle, R. Yvan, Characterization of a high-affinity binding site for the pea albumin 1b entomotoxin in the weevil *Sitophilus oryzae*, *Sitophilus granarius* and *Sitophilus zeamais*, Eur. J. Biochem. 270 (2003) 2429–2435.
[24] B. Delobel, A. Grenier, J. Gueguen, E. Ferrasson, M. Mbailao, Utilisation D'un Plypeptide Derive D'une Albumine PA1b de Legumineuse Comme Insecticide. French Patent 9805877, 1998.
[25] W.S. Abbott, A method of computing the effectiveness of an insecticide, J. Econ. Entomol. 18 (1925) 265–267.
[26] D.J. Finney, Probit Analysis, 3rd ed., Cambridge University Press, London, 1971.
[27] G. Loew, M. Chadwick, D. Smith, Applications of molecular orbital theory to the interpretation of mass spectra. Prediction of primary fragmentation sites inorganic. molecules, Org. Mass Spectrom. 7 (11) (2005) 1241–1251.
[28] A. Somogyi, A. Gomory, K. Vikey, A. Tomas, J. Org. Mass Spectrom. 26 (1991) 936.
[29] C.G. Athanassiou, N.G. Kavallieratos, P. Trematera, Responses of *Sitophilus oryzae* (Coleoptera: Curculionidae) and *Tribolium confusum* (Coleoptera:Tenebrionidae) to traps baited with pheromone and food volatiles, Eur. J. Entomol. 103 (2006) 371–378.
[30] J. Marokhazi, N. Mihala, F. Hudecz, FodorA, L. Graf, I. Venekei, J. Eur. Biochem. Soc. 27 (8) (2007) 1946–1956.
[31] L.H. Heckmann, A. Callaghan, H.L. Hooper, R. Connon, T.H. Hutchinson, S.J. Maund, R.M. Sibly, J. Toxicol. Lett. 172 (3) (2007) 137–145.
[32] A. Lecroise, C. Boulard, B. Keil, Chemical and enzymatic characterization of the collagenase from the insect *Hypoderma lineatum*, J. Eur. Biochem. Soc. 101 (2) (2008) 385–393.
[33] M.D.F. de Meneses, M.A. Rebello, Antiproliferative effect of indomethacin in *Aedes albopictus* (mosquito) cells, Reas. Sci. Med. Biol. Salvador 8 (1) (2009) 14–17.